Cyclic test of buckling restrained braces composed of square steel rods and steel tube

Junhee Park[1], Junho Lee[2] and Jinkoo Kim*[2]

[1]Korea Atomic Energy Research Institute, Daejeon, Republic of Korea
[2]Department of Architectural Engineering, Sungkyunkwan University, Suwon, Korea

Abstract.   In this study total of six buckling-restrained braces (BRBs) were manufactured using a square steel rod as a load-resisting core member and a hollow steel tube as restrainer to prevent global buckling of the core. The gap between the core and the tube was filled with steel rods as filler material. The performances of the proposed BRB from uniaxial and subassemblage tests were compared with those of the specimens filled with mortar. The test results showed that the performance of the BRB with discontinuous steel rods as filler material was not satisfactory, whereas the BRBs with continuous steel rods as filler material showed good performance when the external tubes were strong enough against buckling. It was observed that the buckling strength of the external tube of the BRBs filled with steel rods needs to be at least twice as high as that of the BRBs filled with mortar to ensure high cumulative plastic deformation of the BRB.

Keywords: buckling-restrained braces; seismic performance; uniaxial tests; subassembalge tests.

1. Introductions

The buckling restrained braces (BRBs), which can yield during both tension and compression, have acceptance in many countries around the world. Based on the satisfactory performance obtained from various experiments, BRBs have been actively applied to seismic design and retrofit of building structures in high seismic regions, such as Taiwan, Japan, and United States. Huang *et al.* (2000) carried out static and dynamic loading tests on structures with BRB and showed that the energy dissipation capacity of a frame increased with the installation of BRB, and that the main frame remained elastic even when it was subjected to large earthquake load. Black *et al.* (2002) carried out stability analysis against flexural and torsional buckling of BRB, and presented test results of five BRBs with various configurations. Their study concluded that BRB is a reliable and practical alternative to conventional lateral load resisting systems. Merritt *et al.* (2003) carried out performance tests of BRBs composed of steel cores and external tubes filled with concrete, and found that they behaved stably under cyclic loads, dissipating large amount of hysteretic energy. Tsai *et al.* (2004) proposed a double-Tee double-tube BRB in order to obtain easy-connection configuration, which were applied to seismic retrofit of real structures. Iwata and Murai (2006) developed a buckling-restrained brace formed by welding a core plate covered with unbonded material to a pair of mortar-filled channel steels. Tremblay *et al.*

(2006) performed subassemblage seismic tests on the conventional concrete-filled buckling-restrained braces and the BRB composed of steel core restrained by hollow steel sections, and found that the BRB's exhibited good performance under the quasi-static and dynamic loading sequences. Ding *et al.* (2009) carried out quasi-static tests of BRB encased in reinforced concrete panel, and found out that all specimens exhibited a stable performance under the quasi-static loading until local failure of the panel occurred by either flexure or punching shear. Farhat *et al.* (2009) proposed a systematic methodology for determining the optimal cross-sectional area of BRB using genetic algorithm. Kim *et al.* (2009) investigated seismic performance factors, such as overstrength, ductility, and response modification factors, of buckling-restrained braced frames using nonlinear static pushover analysis and nonlinear dynamic analysis. D'Aniello *et al.* (2008) tested a detachable BRB made of a rectangular steel plate encased in a bolted restraining steel sleeve, and proposed local details and geometrical proportions in order to improve the robustness of the BRB. Pekcan *et al.* (2009) proposed an energy-based design methodology which incorporates BRB in a special truss moment frames as energy dissipation devices. Deulkar *et al.* (2010) investigated the effect of BRB design parameters such as overall length and cross-sectional area of yielding core and proposed a new brace configuration for BRB. Recently Shin *et al.* (2012) carried out sub-assemblage test of buckling restrained knee braces (BRKB) composed of a core plate and two cover channel sections. The BRKB with the load-displacement relationship obtained from the experiment was applied to low-rise residential building structures with weak first story and the seismic performance was investigated. It was observed that both strength and stiffness increased significantly as a results of installation of the BRKB. For design of structures with BRBs, Kim *et al.* (2004) developed an energy-based design procedure for steel moment frames with BRB. BRB's were also applied to seismic design and upgrading of steel bridges (Usami *et al.* 2005, Carden *et al.* 2006).

To accomodate the application of BRBs and to provide basic requirements for the seismic design of buckling-restrained braced frames (BRBFs), AISC (American Institute of Steel Construction) and SEAOC (Structural Engineers Association of California) proposed the Recommended Provision for Buckling-Restrained Braced Frames (2001). This was later adapted to the NEHRP Recommended Provisions for Seismic Regulations for New Buildings and Other Structures (FEMA-450 2004) and to the AISC Seismic Provisions for Structural Steel Buildings (2005), which provides detailed guidelines for design and seismic performance testing of BRB.

This paper presents an experimental study to assess the seismic performance of all-steel buckling-restrained braces made of square steel rod core and hollow steel tube. The gap between the core and the restraining tube was filled with steel rods as filler material. Total of six full scale specimens of BRBs were manufactured and their performances under cyclic load were investigated by both uniaxial and subassemblage tests. Compared with the conventional BRBs filled with concrete, the all steel BRBs presented in this study have advantages in that they can be manufactured without concrete and thus reducing the time and facility required for manufacture. Also as the core elements are made of square steel rods, the overall size of the BRB can be minimized.

2. Design of test specimens and experimental setup

2.1 Design of test specimens

Buckling restrained braces were developed in Japan mainly to provide hysteresis damping for earthquake loading, keeping columns and beams in elastic regions (Wada *et al.* 1992, Iwata 2004). In
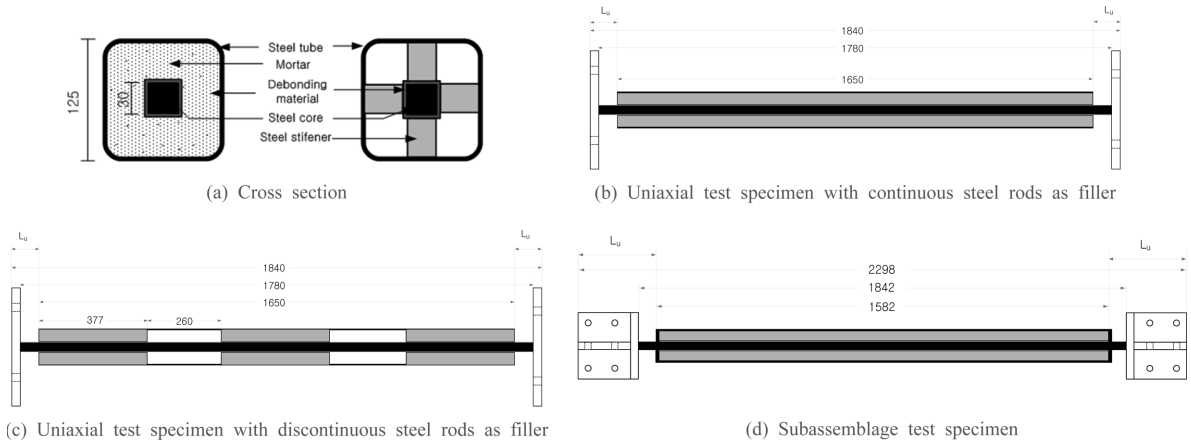
(a) Cross section

(b) Uniaxial test specimen with continuous steel rods as filler

(c) Uniaxial test specimen with discontinuous steel rods as filler

(d) Subassemblage test specimen

Fig. 1 Shape and dimencion of test specimens (mm)

the United States buckling restrained braces are generally designed as parts of seismic load resisting elements (AISC 2005). The test specimens investigated in this study were designed following the guidelines of the AISC Seismic Provisions as chevron braces to be installed in a frame with 6 m span length and 3 m story height. The test specimens, made of SS400 steel ($F_y = 235$ MPa), are composed of a steel core element, a steel external tube, and filler material between the exterior tube and the core rod, as shown in Fig. 1(a). The square rod core element was designed to resist all axial force and the exterior tube and the filler material function to prevent local and global buckling of the core element. As main filler material, both continuous and discontinuous square steel rods were used. For comparison, two specimens filled with mortar were also prepared. The sizes of the core elements were decided considering the maximum capacity of the actuator. The dimensions of the external tubes were determined so that they would not buckle before the core elements yield. The Seismic Provisions recommend that brace connections and adjoining members need to be designed to resist yielding and buckling due to the forces calculated based on the adjusted brace strength obtained as $\beta\omega R_y P_{ysc}$ for compression and $\omega R_y P_{ysc}$ for tension, where β is the compression strength adjustment factor, ω is the strain hardening adjustment factor, R_y is the ratio of the expected yield stress to the specified minimum yield stress, and P_{ysc} is the axial yield strength of steel core. The each end of core elements of the uniaxial test specimens were welded to the square steel plates, as shown in Fig. 1(b), which were connected to the zigs. The ends of the specimens for subassemblage test were welded to gusset plates as shown in Fig. 1(d). To prevent buckling of the connecting parts, Tsai *et al.* (2004) proposed the following relationship

$$P_{e\_trans} = \frac{\pi^2 EI_{trans}}{(KL_u)^2} \geq P_{max} \tag{1}$$

where I_{trans} is the second moment of inertia of the core element in the connection part, L_u is the length of the unrestrained part of the connection, K is the effective length factor, and P_{max} is the maximum compressive strength of the core segment. In this study the effective length factor of 2.0 was used for conservative design of the connection.

The size and thickness of the restraining tubes were determined based on Watanabe *et al.* (1988), who

Table 1 Dimensions of test specimens (unit: mm)

Specimens	Filler	Continuity of filler	Core	Length of core elements	External tubes	Length of tubes	Strength ratios (Pe/Py)
A-1	Square rod	Continuous	30×30	1780	125×125×6	1650	3.76
A-2	Mortar	Continuous	30×30	1780	125×125×3.2	1650	2.21
A-3	Square rod	Continuous	30×30	1780	125×125×3.2	1650	2.21
A-4	Square rod	Discontinuous	30×30	1780	125×125×3.2	1650	2.21
B-1	Square rod	Continuous	28×28	1842	125×125×6	1582	4.76
B-2	Mortar	Continuous	28×28	1842	125×125×6	1582	4.76

Table 2 Results of coupon test

Coupon	Thickness	Width	Yield strength	Ultimate strength	Yield stress	Ultimate stress	Elongation ratio
Unit	mm		kN		kN/mm²		%
Gusset plate	12	20	68.6	80.0	0.286	0.333	34.7
Brace core	12	20	64.2	101.6	0.268	0.423	31.0

proposed that the elastic buckling strength of an external tube of a BRB, P_e, needs to be at least 1.5 times the yield strength of a core element, P_y
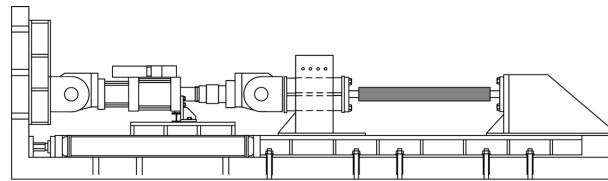
$$\frac{P_e}{P_y} \geq 1.5 \tag{2}$$

The test specimens used in this study have the tube/core strength ratio ranging from 2.21 to 4.76 as shown in Table 1, which also shows the shapes and dimensions of the test specimens. Four specimens (A-1 to A-4) were manufactured with 30 mm × 30 mm steel cores for uniaxial tests and two specimens (B-1 and B-2) with 28 mm × 28 mm steel cores were prepared for subassemblage tests. In the specimens A-2 and B-2 mortar was used as filler material for comparison with the specimens with steel rods as fillers. In the specimen A-4 a set of four short square rods instead of continuous rods were placed at each end and in the middle of the specimen as fillers. The specimens A-1, B-1, and B-2 have thicker external tubes ($t = 6$ mm) than the other specimens ($t = 3.2$ mm). 2 mm-thick rubber sheets were placed between the core and the filler rods to accommodate the transverse deformation due to Poisson's effect. Table 2 presents the coupon test results of the core elements and gusset plates.
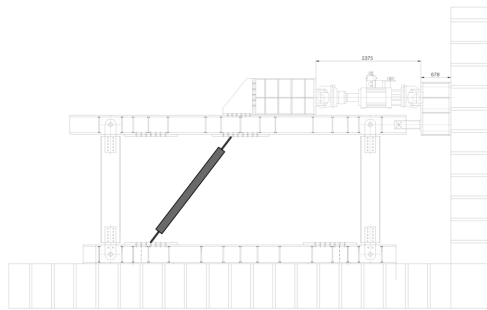
2.2 Test setup and loading protocol

It is stated in the Commentary of Seismic Provisions (2005) that the design of buckling-restrained brace frames require reference to successful tests of a similarly sized test specimen and of a brace subassemblage that includes rotational demands. The former is a uniaxial test intended to demonstrate adequate brace hysteretic behavior, and the latter intended to verify the general brace design concept and demonstrate that the rotations associated with frame deformations do not cause failure of the steel core projection, binding of the steel core to the casing, or otherwise compromise the brace hysteretic behavior.

Fig. 2(a) shows the uniaxial test setup for the A-type BRB specimens, and Fig. 2(b) depicts the subassemblage test setup for the B-type BRB placed in a 5.87 m × 2.93 m loading frame. The test

(a) Uniaxial tests

(b) Framed tests

Fig. 2 Description of test setup

(a) Uniaxial tests   (b) Subassemblage tests

Fig. 3 Photograph of test setup

frame has hinged connections so that the BRB specimen resists all lateral load imposed by the actuator. The actuators used in the uniaxial and the subassemblage tests have the capacity of 1000 kN and 500 kN, respectively. Fig. 3 shows the photograph of the test setups for uniaxial and subassemblage tests.

Fig. 4 depicts the placement of strain gauges to measure deformation and stress states of the core and the external tubes. In the specimen A-4 with discontinuous filler rods, the strain gauges were attached both on the core and the external tube. However in the other specimens filled with continuous filler rods or mortar the gauges were placed only on the external tubes. The axial deformations of the specimens were measured by a linear variable differential transformer (LVDT).

To estimate seismic performance of the specimens, the loading protocol presented in the AISC Seismic Provision for Structural Steel Buildings (2005) and shown in Fig. 5 was imposed on the loading frame. The loading sequence was developed based on a series of nonlinear time history
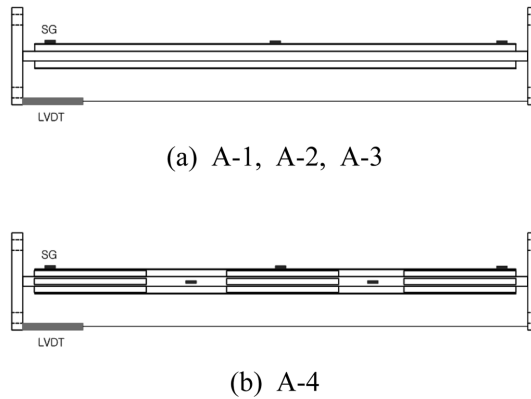
(a) A-1, A-2, A-3

(b) A-4

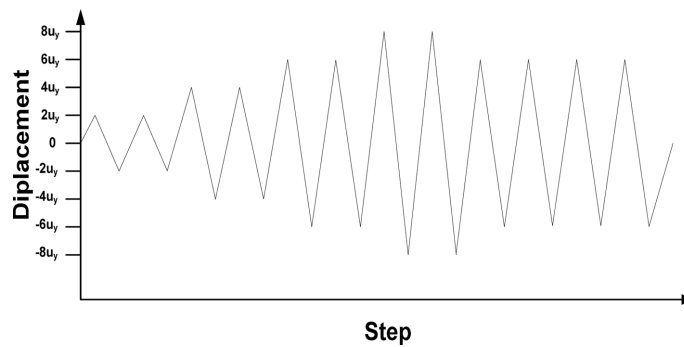Fig. 4 Locations of strain gages

Fig. 5 Loading protocol for cyclic tests

analyses of steel moment frame structures subjected to a range of seismic inputs. The loading protocol imposes maximum brace deformation corresponding to the 3% of the story drift ratio (lateral drift divided by the story height), which is larger than the maximum design drift (Δ_{bm}) stipulated in the AISC Seismic Provision. At the end of the load sequency the cumulative plastic deformation is 208 U_y. The speed of loading was set to be 0.2 mm/sec, and after the specified loading cycles were over, the displacement was gradually increased until failure.

3. Test results

3.1 Failure modes of specimens

Figs. 6~11 show the failure modes of the specimens. The specimen A-1, which was designed with steel rods as filler and with external tube thicker than those of the other A-type specimens, behaved stably until the axial deformation of 13 times the yield deformation (13 u_y) was reached. Fig. 6(a) shows that yield line formed at the end of the core at the axial deformation of six times yield deformation, and Fig. 6(b) depicts the fracture at welding. The strength ratio of the buckling strength of the external tube and the yield strength of the core element is 3.76 in the specimen A-1 as shown in

(a) Formation of yield line at 8u$_y$ (b) Fracture at welding at 13u$_y$

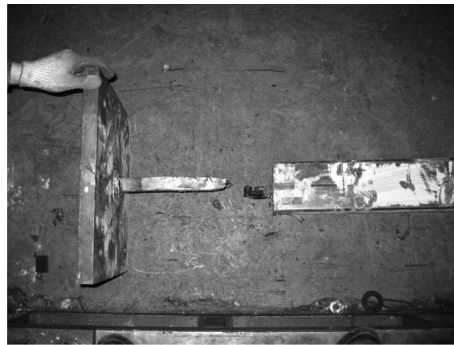Fig. 6 Failure mode of the specimen A-1

Fig. 7 Fracture of core at 13 u$_y$ in specimen A-2

(a) At 6u$_y$ (comp.)   (b) At 8u$_y$ (comp.)   (c) At 6u$_y$ (tension)

Fig. 8 Failure mode of the specimen A-3

Table 1. The specimen A-2 filled with mortar showed ductile behavior similar to the specimen A-1 even though thinner external tube was used, and at tensile loading cycle of 13 times the yield deformation (13 u$_y$) the core element fractured as shown in Fig. 7. The specimen A-3, which is composed of the same core and external tube with the specimen A-2 but is filled with continuous filler rods instead of mortar, failed prematurely as a result of buckling of core element. This implies that the strength ratio of 2.21 may not be large enough for BRB filled with steel rods at four sides of a square rod core element. As depicted in Fig. 8, the core bended significantly at 6 u$_y$. At compression loading cycle in axial deformation of 8 u$_y$ the external tube deformed significantly due to buckling of the core, and at the next tensile loading cycle facture occurred at the core-end plate welding. Fig. 9 shows that local buckling occurred at the external tube of the specimen A-4, which is filled with discontinuous square rods, at the compressive loading cycle corresponding to the four times the yield deformation.
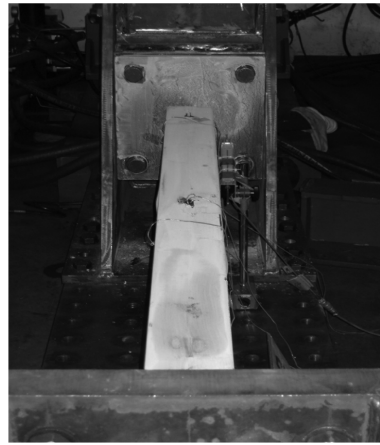
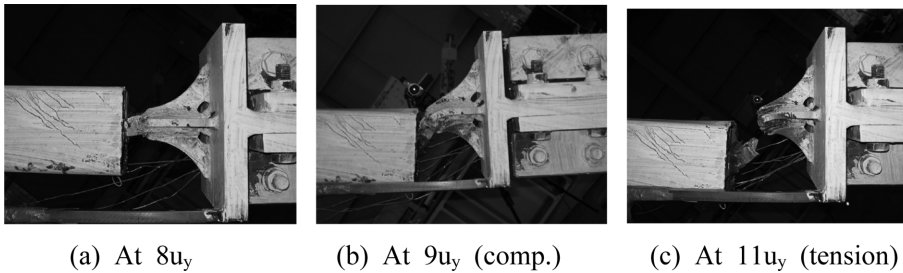Fig. 9 Local buckling at external tube in specimen A-4

(a) At $8u_y$ (b) At $9u_y$ (comp.)   (c) At $11u_y$ (tension)

Fig. 10 Failure mode of the specimen B-1

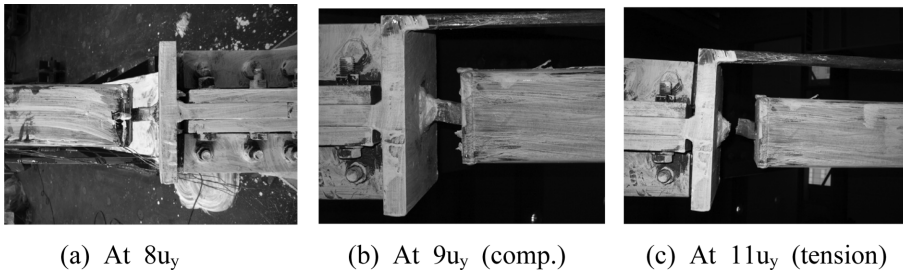(a) At $8u_y$ (b) At $9u_y$ (comp.)   (c) At $11u_y$ (tension)

Fig. 11 Failure mode of the specimen B-2

The specimen fractured at the following tensile loading cycle. The strength ratio of the external tube and the core element of the specimen is the same as those of the specimens A-2 and A-3. Figs. 11 and 12 show the failure modes of the specimens B-1 and B-2 filled with continuous steel rods and mortar, respectively, tested as a part of chevron braces in the steel frame. It can be observed that both the specimens showed similar failure modes. At $8\,u_y$ the core elements bended under compression and at $11\,u_y$ the core elements fractured under tension.

3.2 Hysteretic behavior

Fig. 12 presents the hysteresis curves of the specimens obtained by cyclic loading tests. The vertical axis represents the axial load in the core normalized by the nominal yield force of the core element, and the horizontal axis represents the axial displacement of the core. The specimens A-3 and A-4 in which square rods were used as filler material with relatively thin external steel tubes failed by buckling of core elements before the full loading cycles were completed. Especially the specimen A-4 with discontinuous filler rods did not finish 6th loading cycles. The other four specimens behaved stably both under tension and compression until all the specified loading cycles were completed. After the loading cycles were over, the specimens for uniaxial tests A-1 and A-2 failed at axial deformation of $12\,u_y$, whereas the specimens for subassemblage test, B-1 and B-2, failed at smaller axial deformation of $9\,u_y$ and $10\,u_y$, respectively. The specimens A-2 and A-3 have the same cross-sectional dimensions and the same strength ratio of 2.21 but have different filler materials. The specimen A-2 filled with mortar behaved stably until the specified loading cycles were finished and failed by fracture of the core, whereas the specimen A-3 with square rods as filler material failed prematurely due to buckling of core element. Even though the strength ratio of the specimen A-3 is larger than the value suggested by Watanabe *et al.* (1988), the external tube combined with the filler steel rods could not prevent buckling of the core element. On the other hand the specimen A-2 filled with mortar showed successful performance under the specified loading protocol. The specimen A-1 with square rods as filler material but with thicker exterior tube behaved similarly to the specimen A-2 which is filled with mortar but has thinner exterior steel tube. Therefore it may be concluded that when only the four sides of the core are filled with steel rods, external tube with larger buckling strength is required than when mortar is used as

(a) A-1   (b) A-2   (c) A-3
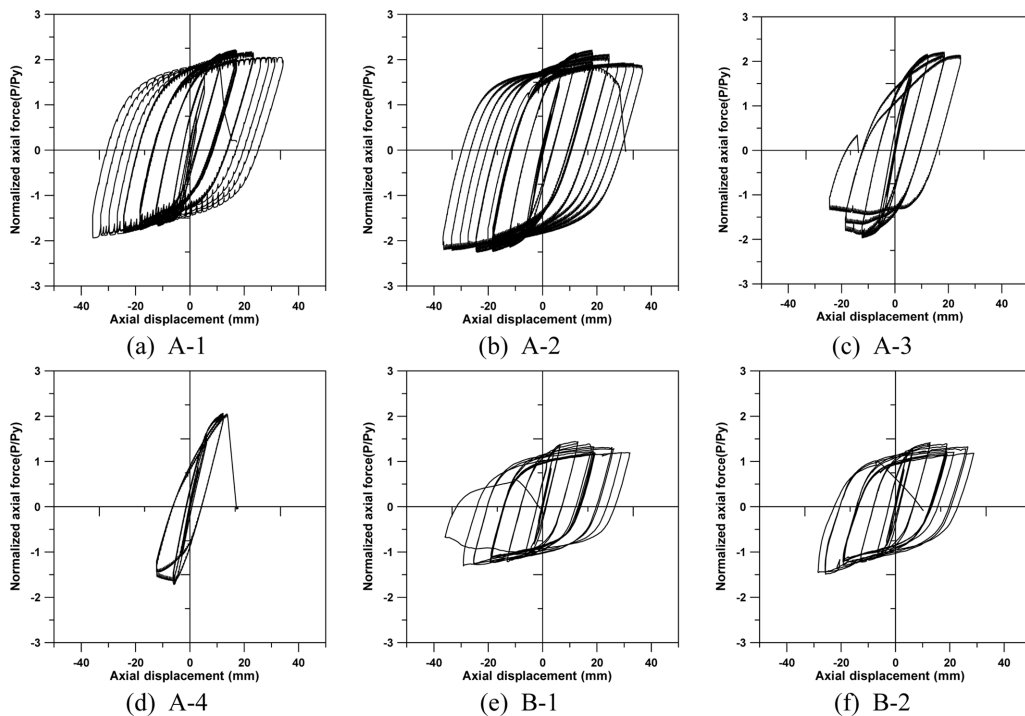
(d) A-4   (e) B-1   (f) B-2

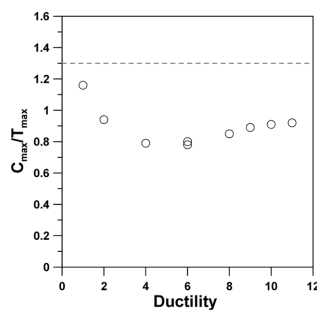Fig. 12 Hysteresis loops of test specimens

filler material. The performance of the specimen A-1 demonstrates that the strength ratio of 3.76 is enough to guarantee ductile behavior of BRB filled with steel rods. The specimens for subassemblage test, B-1 and B-2, were designed to have higher strength ratio of 4.76 considering that shear forces as well as axial forces are applied to the specimens. It can be observed that both specimens showed stable behavior under the loading protocol.

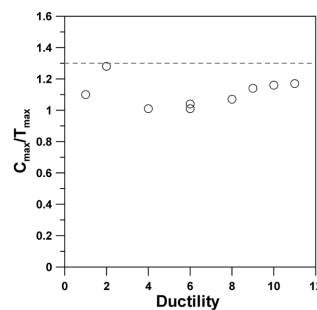### 3.3 Compression strength adjustment factor and cumulative plastic deformation

When BRBs are placed between stories as inverted V shaped braces, vertical unbalanced force may occur if tensile strength of BRB is not equal to compressive strength. The SEAOC-AISC Recommended Provisions for BRBFs (2001) recommends that the compression strength adjustment factor, which is the ratio of the compressive and tensile strengths, shall be less than 1.3 to prevent large unbalanced force. Table 3 tabulates the adjustment factor of the specimen A-2 at each loading cycle, where it can be observed that the ratio of the compressive to tensile strength in each loading cycle is less than the recommended value of 1.3. Fig. 13 compares the compressive to tensile strength ratios of the specimens A-1 and A-2. Both specimens showed stable hysteretic behavior under the specified load and the strength ratios turned out to be less than 1.3. It can be observed that the strength ratios of the

Table 3 Loading history (A-2)

Loading cycle	Tension (T, kN)	Compression (C, kN)	Ratio (C/T)
U_y	197.0	216.8	1.10
$2\,U_y$	357.4	457.6	1.28
$4\,U_y$	513.8	516.6	1.01
$6\,U_y$	532.8	539.8	1.01
$8\,U_y$	507.4	544.0	1.07
$6\,U_y$	454.6	474.4	1.04
$9\,U_y$	454.6	518.8	1.14
$10\,U_y$	463.0	535.6	1.16
$11\,U_y$	461.0	539.8	1.17
$12\,U_y$	446.2	535.6	1.20
$13\,U_y$		Core failure	

(a) A-1   (b) A-2

Fig. 13 Compressive strength adjustment factors of the test specimens

Table 4 Cumulative ductility ratio

Loading cycle	Specimens					
	A-1	A-2	A-3	A-4	B-1	B-2
U_y	0.0	0.0	0.0	0.0	0.0	0.0
$2\,U_y$	8.0	8.0	8.0	8.0	8.0	8.0
$4\,U_y$	32.0	32.0	32.0	32.0	32.0	32.0
$6\,U_y$	72.0	72.0	72.0	36.4	72.0	72.0
$8\,U_y$	128.0	128.0	90.9		128.0	128.0
$6\,U_y$	**208.0**	**208.0**			**208.0**	**208.0**
$9\,U_y$	240.0	240.0			240.0	240.0
$10\,U_y$	276.0	276.0			276.0	276.0
$11\,U_y$	316.0	316.0			284.8	283.32
$12\,U_y$	360.0	360.0				
$13\,U_y$	375.0	381.2				

specimen A-2, which is filled with mortar, are larger than 1.0 in all loading cycles, whereas the strength ratios of the specimen A-1 filled with four square steel rods are less than 1.0 in some loading cycles. This implies that slight bending deformation of core element occurred in the specimen filled with steel rods when subjected to compression. On the other hand the core of the specimen in which the gap between the core and the external tube is completely filled with mortar is subjected only to axial deformation.

Table 4 presents the cumulative plastic deformation (CPD) of the specimens at each loading cycle. The CPD is the summation of the difference between the maximum compressive displacement (u_{pi}^{max}) and the maximum tensile displacement (u_{pi}^{min}) divided by the yield displacement in each loading cycle

$$CPD = \sum_i \frac{\left| u_{pi}^{max} - u_{pi}^{min} \right|}{u_y} \tag{3}$$

The yield displacements u_y of the specimens A-1 to A-4 are 3.05 mm, and those of the specimens B-1 and B-2 are 3.16 mm. The AISC Recommended Provisions for Buckling-Restrained Braced Frames (2001) specifies the minimum CPD of 200 for BRB. It can be observed in Table 4 that the CPD of the specimens A-1 and A-2, which showed stable hysteretic behavior until the specified loading sequence was over, reached 375 and 381, respectively, exceeding the minimum requirement by 88% and 91%, respectively. The subassemblage test specimens B-1 and B-2 experienced cumulative plastic deformations as large as 280 before failure exceeding the minimum requirement by 40%. However the specimens A-3 and A-4 which failed before the loading sequence was completed showed CPD less than half the required value.

3.4 Measured strain

Fig. 14 depicts the strain time histories of the uniaxial test specimens, where the dotted horizontal lines denote the yield strain. It can be observed in Fig. 14(a) that the strain of the external tube of the specimen A-1 is almost negligible, which implies that only the core element deforms and the external tube does not participate in resisting the axial force imposed on the BRB. However, as can be noticed in

(a) A-1 (Ext. tube)

(b) A-3 (Ext. tube)
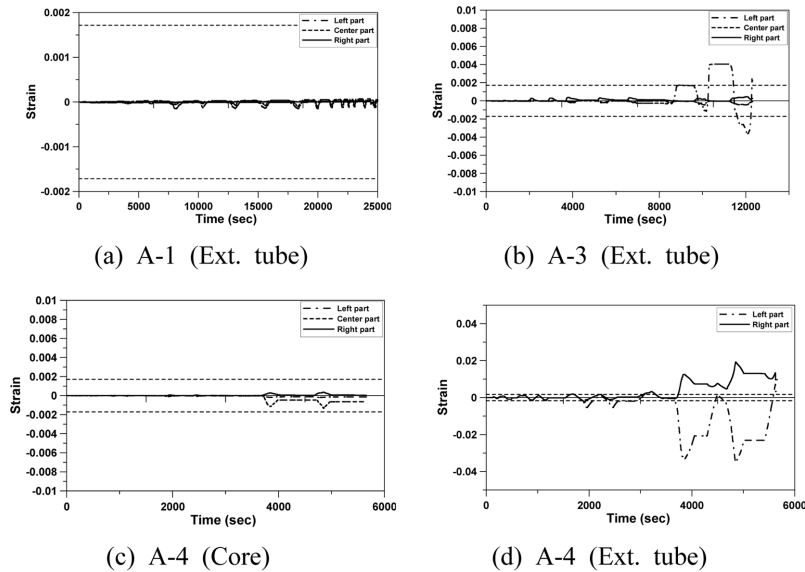
(c) A-4 (Core)

(d) A-4 (Ext. tube)

Fig. 14 Strain time histories of test specimens

Fig. 14(b) and 14(d), significant axial deformations occurred in the external tubes of the specimens A-3 and A-4, which failed prematurely. From the strain measured in the core and the external tube of the specimen A-4, plotted in Fig. 14 (c) and (d), respectively, it can be observed that strain in the tube increased significantly when the core element buckled under compression.

4. Conclusions

In this study total of six buckling-restrained braces (BRBs) were manufactured using a square steel rod as a load-resisting core member and a hollow steel tube as restrainer were investigated by uniaxial and subassemblage tests. The gap between the core and the tube was filled with steel rods or mortar as filler material, and their performances of BRBs with different filler materials were compared.

The test results showed that the performance of the BRB with discontinuous steel rods as filler material between the core and the external tube was not satisfactory, whereas the BRBs filled with mortar showed stable hysteretic behavior and large cumulative plastic deformation when they were subjected to the loading protocol recommended by the AISC Seismic Provisions. When continuous steel rods were used as filler material, the specimens with exterior tube thicker than that of the specimen filled with mortar showed equivalent strength and ductility. The ratios of the compressive to tensile strength of all specimens turned out to be less than the recommended value of 1.3. The cumulative plastic deformation of the specimens except the specimens with discontinuous filler rods or with relatively thinner exterior tube exceeded the specified minimum requirement. Based on the test results it was concluded that high cumulative plastic deformation and energy dissipation equivalent of the conventional BRB could be achieved when higher thickness of the external restraining tube is used in the BRB with continuous steel bars as filler material.

The all-steel BRBs proposed in this study have advantage in that they can be made without using

concrete as filler material and therefore saving significant time and facility required for mixing and cure of concrete. In addition as the core elements are made of square steel rods, the overall size of the BRB may be minimized.

Acknowledgement

References

AISC. (2005), *Seismic Provisions for Structural Steel Buildings*, American Inst. of Steel Construction, Inc., Chicago.

AISC-SEAOC. (2001), Recommended Provisions for Buckling-Restrained Braced Frames, American Inst. of Steel Construction, Inc., Chicago.

Black, C., Makris, N. and Aiken, I. (2001), Component testing, stability analysis and characterization of buckling restrained braces, Final report to Nippon Steel Corporation.

Carden, L. P., Itani, A.M. and Buckle, I. G. (2006), "Seismic performance of steel girder bridges with ductile cross frames using buckling-restrained braces", *J. Struct. Eng.*, **132**(3), 338-345.

Deulkar, W. N., Modhera, C. D. and Patil, H. S. (2010). Buckling restrained braces for vibration control of building structure, *International Journal of Research and Reviews in Applied Sciences*, **4**(4), 363-372.

D'Aniello, M., Della Corte, G. and Mazzolani, F. M. (2008), Only-steel buckling restrained braces. 5th European Conference on Steel and Composite Structures, Graz, Austria.

Ding, Y., Zang, Y. and Zhao, J. (2009), Tests of hysteretic behavior for unbonded steel plate brace encased in reinforced concrete panel, *J. Constr. Steel Res.*, **65**(5), 1160-1170.

Farhat, F., Nakamura, S. and Takahashi, K. (2009), Application of genetic algorithm to optimization of buckling restrained braces for seismic upgrading of existing structures, *Comput. Struct.*, **87**(1-2), 110-119.

Huang, Y. H., Wada, A., Sugihara, H., Narikawa, M., Takeuchi, T. and Iwata, M. (2000), "Seismic performance of moment resistant steel frame with hysteretic damper", The Third International Conference STESSA, Montreal, Canada.

Iwata, M. (2004), Applications-Design of Buckling Restrained Braces in Japan, 13th World Conference on Earthquake Engineering, Vancouver, B.C., Canada.

Iwata, M. and Murai, M. (2006), Buckling-restrained brace using steel mortar planks; performance evaluation as a hysteretic damper, *Earthq. Engng. Struct. Dyn.*, **35**(14), 1807-1826.

Kim, J., Choi, H. and Chung, L. (2004), "Energy-based seismic design of structures with buckling-restrained braces", *Steel. Compos. Struct.*, **4**(6), 437-452.

Kim, J., Park, J. and Kim, S. (2009), "Seismic behavior factors of buckling-restrained braced frames," *Struct. Eng. Mech.*, **33**(3), 261-284.

Merritt, S., Uang, C. M. and Benzoni, G. (2003), *Subassemblage testing of corebrace buckling-restrained braces*, Final report to CoreBrace, LLC, Department of Structural Engineering, University of California, San Diego.

Pekcan, G., Linke, C. and Itani, A. (2009), Damage avoidance design of special truss moment frames with energy dissipating devices, *J. Constr. Steel Res.*, **65**, 1374-1384

Shin, J., Lee, K., Jeong, S., Lee, H. and Kim, J. (2012), Experimental and analytical studies on buckling-restrained knee braceing systems with channel sections, *Int. J. Steel Struct.*, **12**(1), 93-106

Tremblay, R., Degrange, D. and Blouin, J. (1999), Seismic rehabilitation of a four-story building with a stiffened bracing system, Proceeding of the 8th Canadian Conference on Earthquake Engineering, Vancouver.

Tsai, K. C., Lai, J. W., Hwang, Y. C., Lin, S. L. and Weng, C. H. (2004), "Research and application on double-core buckling restrained braces in Taiwan", Proceeding of the 13th World Conference on Earthquake

Engineering, Paper No. 2179, Vancouver, B.C., Canada.

Usami, T., Lu, Z. and Ge, H. (2005), A seismic upgrading method for steel arch bridges using buckling-restrained braces, *Earthq. Engng. Struct. Dyn*., **34**(4-5), 471-496.

Wada, A., Connor, J. J., Kawai, H., Iwata, M. and Watanabe, A. (1992), Damage Tolerant Structure, Proceedings of Fifth U.S.-Japan Workshop on Improvement of Building Structural Design: ATC-15-4 Report, San Diego, California, 27-39.

Watanabe, A., Hitomoi, Y., Saeki, E., Wada, A. and Fujimoto, M. (1988), "Properties of braced encased in buckling-restrained concrete and steel tube", *Proceedings of Ninth World Conference on Earthquake Engineering*, Tokyo-Kyoto, Japan, Vol. **IV**, 719-724.

CC